Estimates of ocean heat flux at SHEBA

Donald K. Perovich and Bruce Elder
ERDC-CRREL, Hanover, NH, USA

Received 2 October 2001; revised 11 March 2002; accepted 11 March 2002; published 15 May 2002.

[1] Observations of sea ice mass balance and temperature made during the year-long Surface HEat Budget of the Arctic Ocean (SHEBA) field experiment were used to calculate monthly estimates of the ocean heat flux for a variety of ice types. The ocean heat flux displayed a strong seasonal cycle, with values of a few W m^{-2} from October through June followed by a steady increase in June and July. By the end of July the the ocean heat flux for undeformed ice reached a peak value of about 33 W m^{-2} during a period of substantial ice motion. The annual average ocean heat flux for multiyear ice ranged from 7.5 W m^{-2} for undeformed ice to 10.4 W m^{-2} for a melt pond to 12.4 W m^{-2} for an old ridge. Annual averages measured at SHEBA were more than twice as large as values observed in 1975 during AIDJEX. *INDEX TERMS:* 4540 Oceanography: Physical: Ice mechanics and air/sea/ice exchange processes; 1863 Hydrology: Snow and ice (1827); 4572 Oceanography: Physical: Upper ocean processes

1. Introduction

[2] Changes in the thickness and extent of the Arctic sea ice cover may be harbingers of climate change. A key element affecting the mass balance of sea ice is the transfer of heat from the ocean to the underside of the ice, the ocean heat flux [*Maykut and Untersteiner*, 1971; *Maykut*, 1986; *Ebert et al.*, 1995]. Early theoretical work treated the ocean heat flux as a temporally invariant constant equal to 2 W m^{-2}. More recent observational work has shown that this is not the case. Analyzing observations made in the Beaufort Sea in 1975 during the Arctic Ice Dynamics Joint Experiment, *Maykut and McPhee* [1995] established that there is a strong seasonal dependence of the ocean heat flux (F_w). Examining undeformed multiyear ice, they found peak values as large as 40 W m^{-2} in summer and an annual average of 3 to 5 W m^{-2}. Observations by *Perovich et al.* [1997], in the Beaufort Sea in 1993–1994, determined that for undeformed ice the annual average of the ocean heat flux was 4 W m^{-2}, and the summer average was 9 W m^{-2}. A comprehensive study by *Wettlaufer* [1991] in the eastern Arctic revealed that, even on the small scale of a few hundred meters, there is considerable spatial variability in the ocean heat and that F_w is strongly influenced by ocean water masses.

[3] The ocean heat flux can be determined, with difficulty, from direct measurements of the vertical eddy flux of sensible heat [*McPhee*, 1992; *Maykut and McPhee*, 1995]. This entails measuring times series of vertical profiles of ocean temperature, salinity, and current, as well as estimating ice bottom roughness. Temporally averaged values of F_w can also be determined from relatively simple measurements of ice temperature and mass balance [*McPhee and Untersteiner*, 1982; *Perovich et al.*, 1989; *Wettlaufer*, 1991; *Perovich et al.*, 1997]. Ice temperature and mass balance measurements were made as part of the year-long SHEBA (Surface HEat Budget of the Arctic Ocean) field experiment [*Moritz et al.*, 1993; *Perovich et al.*, 1999; *Uttal et al.*, 2002]. This experiment lasted from October 1997 through October 1998 and was directed at acquiring a high-quality, comprehensive, integrated dataset that defined the state of the atmosphere, ice, and ocean over an entire annual cycle [*Perovich et al.*, 1999]. During the experiment the ice camp was a Lagrangian drifter moving from 75°N, 142°W to 80°N, 116°W. This platform provided an excellent opportunity to investigate the temporal evolution of F_w over an annual cycle for a variety of sea ice types including first year ice, ponded multiyear ice, undeformed multiyear ice, and an old multiyear ridge.

2. Observations and Methods

[4] There was an extensive mass balance measurement program during the SHEBA field experiment [*Perovich et al.*, in press]. Five sites had thermistor strings to measure the ice temperature and thickness gauges to measure the ice mass balance. For convenience and consistency in nomenclature, each site was named after a city: Pittsburgh, Quebec, Seattle, Tuk, and Baltimore. The Pittsburgh mass balance site was relatively thick multiyear ice. Quebec was a multiyear hummock with a thin snow cover. In fall 1997 the Seattle mass balance site was an area of ponded multiyear ice with nearby hummocks. Seattle was also heavily ponded in summer 1998. The Tuk mass balance site was an old consolidated ridge that was 3–4 m thick at the beginning of the experiment. The Baltimore mass balance site was first-year ice. Ice at this site started growing in late August 1997 and was about 40 cm thick in mid-October 1997. Baltimore was heavily ponded in the summer of 1998, with many of the ponds melting all the way through to the ocean. The sites were located more than 100 m and less than 5 km from one another.

[5] The instrumentation at each mass balance site consisted of several thickness gauges, a thermistor string, and a datalogger. The thermistor strings were polyvinyl-chloride rods with thermistors spaced at 10-cm intervals. A vertical hole was drilled through the ice, and the thermistor string was installed so that it extended from the air through the snow, through the ice, and into the upper ocean. The accuracy of the thermistors was ±0.1°C. Thermistor measurements were recorded hourly and stored using a Campbell Scientific Inc. CR-10 datalogger. Hot-wire thickness gauges [*Untersteiner*, 1961; *Perovich et al.*, in press] were used to measure ice accretion or ablation at the underside of the ice. Uncertainties in gauge readings were typically less than 0.5 cm. Gauges were read every 1–2 weeks during winter and every 4 days during summer.

[6] Ice temperature profiles, and measurements of ablation/accretion at the ice bottom can be used to calculate the ocean heat flux by treating it as a residual of the conductive (Q_f), specific (Q_s), and latent (Q_L) heats of the ice:

$$F_w = \left(\frac{1}{\Delta t}\right)\left(Q_f + Q_s + Q_L\right) \qquad (1)$$

Q represents heat fluxes integrated over a time period Δt. The sign convention is that cooling, freezing, and upward heat flow are negative, while warming, melting, and downward heat flux are

0094-8276/02/2001GL014171$05.00

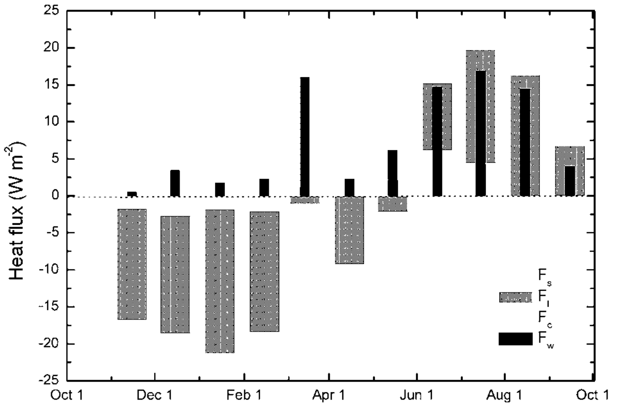

Figure 1. The annual cycle of monthly averages of ocean heat flux for undeformed multiyear ice (Pittsburgh). The shaded bars are the contributions from specific, latent, and conductive fluxes. Negative values represent cooling, freezing, and downward heat conduction. The ocean heat flux is the residual of the other fluxes.

positive. The conductive heat term (Q_f) is the heat flow though a specified reference level within the ice and is equal to

$$Q_f = \int k_s \frac{\partial T}{\partial z} dt \cdot \tag{2}$$

The thermal conductivity of sea ice (k_s) is defined using *Untersteiner* [1961] expression. The time integral in Equation (2) was numerically evaluated using a time step of 1 day. The derivative $\partial T/\partial z$ was determined from a linear fit of observed temperatures across the reference level.

[7] The specific heat (Q_s) is the change in heat content of the ice and is

$$Q_s = \rho \iint c_s dT dz \tag{3}$$

where ρ is the ice density and c_s is the specific heat of sea ice. We used *Schwerdtfeger*'s [1963] expression for the specific heat of sea ice.

[8] The latent heat (Q_L) is

$$Q_L = \rho \int q_m dz. \tag{4}$$

The integrals over dz in equations (3) and (4) are from a reference level in the ice to the bottom of the ice. q_m is the heat needed to melt a parcel of ice and is calculated using *Schwerdtfeger*'s [1963] relationship. Q_s and Q_L were numerically integrated over dz using a spacing of 5 cm.

[9] The expressions for Q_f, Q_s, and Q_L were substituted into Equation (1) to determine F_w. Both Q_L and Q_s depend on salinity, which was a complex and variable function of both position in the ice and time. Ice cores were taken at each thermistor site in the spring, but there was not a complete record of the evolution of the salinity profile near the bottom of the ice. Based on the measured profiles, an average value of 4 o/oo was used to represent the lower portion of the ice at all sites for the entire year. An average value of 900 kg m^{-3} was used for the sea ice density.

[10] The major difficulty in this approach lies in precisely determining the amount of ice growth or melt at the bottom. The uncertainty in the thickness gauge measurements was ±0.5 cm, representing ±1.5 MJ m^{-2}. The approach works best when averaging over long time intervals. For example, based on potential gauge error the uncertainty in ocean heat flux is 17.5 W m^{-2} for daily estimates, 2.5 W m^{-2} for weekly estimates, and 0.6 W m^{-2} for monthly estimates.

3. Results

[11] Results for multiyear ice at the Pittsburgh site are presented in Figure 1. Monthly averages of the specific heat flux ($F_s = Q_s/\Delta t$), latent heat flux ($F_L = Q_L/\Delta t$), and conductive heat flux ($F_f = Q_f/\Delta t$) for the lower portion of the ice are plotted, along with their residual, the ocean heat flux. During much of the winter the ocean heat flux was the small residual of two large numbers of opposite sign: the conductive flux and the latent flux. From January on, the conductive flux continually decreased, becoming negative in June as the upper portion of the ice became slightly warmer than the lower portion. By April the ice began to warm, and the specific heat flux became positive. In June, bottom ablation started, causing a change in the sign of the latent heat flux. In early summer the ice was warming and melting, and F_w was dominated by the specific and latent fluxes. Later in the summer the ice reached its salinity-determined melting point, and F_w was governed by F_l.

[12] The ocean heat flux was small, but not zero, from November through February, with values ranging from 0.5 to 3.4 W m^{-2} and averaging 2.0 W m^{-2}. Surprisingly the monthly average jumped sharply in March to 16 W m^{-2} and just as sharply dropped to 2.3 W m^{-2} in April. From April on, there was a slow, steady increase in F_w, reaching a peak in July of 16.8 W m^{-2}, followed by a decline in August and September. *Maykut and McPhee* [1995], analyzing data from the 1975 AIDJEX program in the Beaufort Sea, reported a similar summer increase in ocean heat flux and attributed it to solar heating of the upper ocean.

[13] Figure 2 presents a more detailed examination of the ocean heat flux at the undeformed multiyear Pittsburgh site from March through October, showing 4- to 8-day, as well as monthly, averages. These 4- to 8-day averages illustrate the signifcant temporal variability of the ocean heat flux. The ocean heat flux was about 5 W m^{-2} in the first half of March, then jumped to 37 W m^{-2}, the maximum F_w observed at Pittsburgh for the entire year. This increase was due to entrainment of warmer, deeper water as the ice station rapidly drifted onto the shallow water of the Chukchi Cap during a storm. This entrainment was evident in an increase in the heat content of the mixed layer under the ice

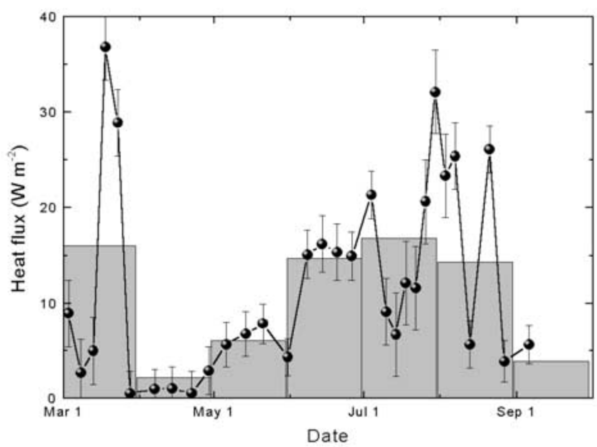

Figure 2. Time series of ocean heat flux measured at Pittsburgh from March through October 1998. Monthly values, values are averaged over 4- to 8-day intervals, and error bars are plotted.

Table 1. Summary of Monthly Values of Ocean Heat Flux

Time interval	Multiyear (Pittsburgh)	Multiyear (Quebec)	Ponded (Seattle)	Ridged (Tuk)	First year (Baltimore)
11/1/97–12/1/97	1	1	3	4	1
12/1/97–1/1/98	3	2	2	10	4
1/1/98–2/1/98	2	7	3	5	2
2/1/98–3/1/98	2	4	5	9	5
3/1/98–4/1/98	16	14	10	14	11
4/1/98–5/1/98	2	3	2	7	1
5/1/98–6/1/98	6	4	2	8	5
6/1/98–7/1/98	15	6	25	13	
7/1/98–8/1/98	17	19	12	33	
8/1/98–9/1/98	14	24	32	28	
9/1/98–10/1/98	4	4	20	4	
Annual average	7.5	7.9	10.4	12.1	

[*Perovich et al.*, 1999]. Ice motion was rapid, as much as 25 km day^{-1}, further enhancing the ocean heat flux. This resulted in bottom melting of the ice, even though air temperatures were as low as −30°C [*Perovich et al.*, in press]. This episode was brief, and F_w quickly dropped to background levels of 2–5 W m^{-2}.

[14] From May through July the monthly averages show a steady monotonic increase in ocean heat flux, but the 4- to 8-day averages reveal a more complex structure with large fluctuations of tens of W m^{-2}. The heat content of the upper ocean mixed layer increased steadily and smoothly from late May through late July in a fashion that was consistent with solar heating [*Maykut and McPhee*, 1995; *Perovich et al.*, 1999; *Uttal et al.*, 2002]. Aside from a brief period at the beginning of June, there was a concomitant increase in F_w from early May until early July. However, in the first half of July, F_w dropped from nearly 20 to about 5 W m^{-2}. Then, in the last week of July, there was a rapid increase in F_w from 10 to 35 W m^{-2}. This variability was a result of changes in ice dynamics. The ocean heat flux is a function of the heat content of the upper ocean and turbulent mixing in the boundary layer [*McPhee*, 1992]. In a simplistic sense we can consider floe speed as a surrogate for turbulent mixing. For much of July, conditions were quiescent and there was little ice motion. Consequently there was a decrease in the ocean heat flux. This changed at the end of the month as a storm hit SHEBA with 8- to 12-m s^{-1} winds. Floe speed increased from 6 cm s^{-1} on 26 July to 43 cm s^{-1} on 29 July (Moritz, personal communication), and the ocean heat flux grew to 35 W m^{-2}.

[15] The peak F_w of 35 W m^{-2} between 27 July and 31 July was followed by a steady decrease during the remainder of the experiment, as there was not enough energy available to sustain these peak heat fluxes. During the ocean heat flux peak, considerable heat was extracted from the mixed layer. Since the incident solar irradiance was steadily waning, this heat was not replaced, so the mixed layer gradually cooled.

[16] This experiment provided the opportunity to transcend earlier efforts and explore the annual cycle of F_w for first year ice, an old ridge and a melt pond. Monthly averages of F_w, determined at five sites, are presented in Table 1 and plotted in Figure 3. The dataset from the first-year ice site is abbreviated since the ice completely melted. The thermistor string at the ridged multiyear site was destroyed by bears at the end of July. To compensate for the missing data, we assumed that F_s was negligible in August and September, and we used the observed July value for F_c.

[17] All sites exhibited the same general behavior: small values during most of the winter, a spike in March, an increase in summer to a maximum at the end of July and beginning of August, followed by a decline in August and September. However, as the plot indicates, there were site-to-site differences in F_w. From November through May the standard deviation of F_w was 2–3 W m^{-2}. The standard deviation increased in summer to 7–9 W m^{-2} in conjunction with the increase in F_w.

[18] Results from the Seattle site are interesting in that it was the only site to exhibit a decrease in F_w in July. This site was heavily ponded, thinner than the other multiyear sites, and only 50 m from a lead. During the quiescent period in July the fresh meltwater runoff from the ice gradually filled the leads, eventually extending below the bottom of thinner ice [Pegau, pers. comm.; *Richter-Menge et al.*, 2001]. This meltwater was strongly stably buoyant and insulated the ice from heat in the mixed layer. In addition, at the Seattle site in late July, an ice layer formed at the meltwater-seawater interface effectively reducing F_w at the ice bottom to zero [*Perovich et al.*, in press].

[19] There was a sharp increase in F_w at the Seattle site in August, as well as a continued increase at the Quebec site. Mixing due to increased ice motion erased the stable surface layer at Seattle. Also, after the main SHEBA floe broke up during the divergence event in late July [*Richter-Menge et al.*, 2001], the Quebec and Seattle sites were at the edges of floes. The sites were thus close to the heat source of relatively warm lead water at a time when this water was being mixed under the ice (Pegau, in press), resulting in a local enhancement of F_w. The other sites were at least a few hundred meters from the floe edge.

[20] The annual average of the ocean heat flux was quite similar for the multiyear sites: 7.5 W m^{-2} for Pittsburgh and 7.9 W m^{-2} for Quebec. For the ponded ice at Seattle, the annual average was 10.4 W m^{-2}. The enhanced annual average at Seattle was the result of higher summer values of F_w, which were due to the nearby presence of a lead. The largest annual average ocean heat flux was 12.1 W m^{-2} for the old ridge at Tuk. This provides quantitative support for the commonly accepted belief that ridge keels are areas of enhanced ocean heat flux [*Maykut and McPhee*, 1995].

[21] Earlier measurements of ocean heat flux in the Beaufort Sea using the mass balance method have yielded annual averages of 3.5 W m^{-2} in 1975 [AIDJEX; *Maykut and McPhee*, 1995] and 4.0 W m^{-2} in 1993–1994 [*Perovich et al.*, 1997]. The SHEBA values are two to three times larger than these prior results. The earlier experiments did not have any mid-winter peaks in ocean heat flux. However, the March 1998 F_w peak only increased the annual average by about 1 W m^{-2}. The heat source of the relatively large ocean flux observed at SHEBA is not yet established. *Maykut and McPhee* [1995] determined that solar radiation input to the upper ocean through leads was the primary energy source of the ocean heat flux. However, SHEBA lead fractions were smaller [*Perovich et al.*, in press] than those measured at

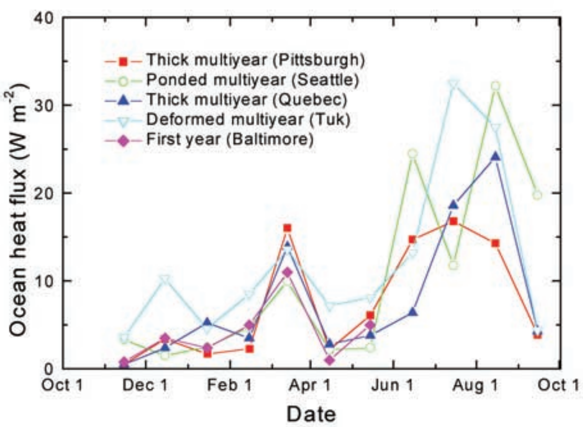

Figure 3. Time series of monthly values of ocean heat flux determined at five sites: thick multiyear ice (Pittsburgh and Quebec), ponded multiyear ice (Seattle), ridged multiyear ice (Tuk), and first-year ice (Baltimore).

AIDJEX, even though the ocean heat flux was much larger. The June through August ocean heat transfer to the bottom of undeformed multiyear ice was 153 MJ m^{-2}, representing 10% of the total solar radiation incident on the ice cover. We estimate that approximately two-thirds of this energy (110 MJ m^{-2}) was input to the ocean through leads, and some of this lead energy was lost to lateral melting of the ice floes [*Perovich et al.*, in press]. Thus at SHEBA there must have been an additional source of heat that contributed to F_w. Because of the initially thin ice cover and large amount of summer ablation [*Perovich et al.*, 1999], SHEBA had a larger areal coverage of melt ponds and had ice that was substantially thinner than AIDJEX. For the SHEBA ice conditions, significant amounts of solar radiation were transmitted to the ocean through ponds and bare, thin ice. This is a potential positive feedback mechanism, where thinning ice leads to increased solar radiation transmitted to the ocean, resulting in larger values of F_w and enhanced bottom melting. Future work needs to quantify the contribution of solar radiation transmitted through the ice to the ocean heat flux.

4. Conclusions

[22] Temporally averaged values of ocean heat flux were determined over an annual cycle using ice temperature and mass balance data measured during the SHEBA field experiment. The ocean heat flux exhibited a strong seasonal dependence. With one brief exception, F_w was only a few W m^{-2} from November until May. The exception was a storm- and topography-induced upwelling event in March, when the five-day average of F_w reached 37 W m^{-2}. Starting in May, there was a steady increase in the ocean heat flux, reaching a peak in late July and early August. There was significant variability in F_w for different multiyear ice types. The value of 12.1 W m^{-2} for an old ridge was the largest annual average F_w, compared to 7.5 W m^{-2} for undeformed ice and 10.4 W m^{-2} for a melt pond. Peak monthly averages in summer were about 18 W m^{-2} for undeformed multiyear ice and 32 W m^{-2} for ponded ice and ridged ice. Values of F_w observed during SHEBA were more than twice as large as those measured in 1975 during AIDJEX. Indications are that solar radiation transmitted through the extensive ponds and the relatively thin bare ice at SHEBA contributed substantially to the ocean heat flux.

[23] **Acknowledgments.** The authors thank H. Bosworth and J. Richter-Menge for their capable assistance during the SHEBA deployment phase. We also thank the crew of the *Des Groseilliers* and the SHEBA Logistics Office for their excellent support. This work was funded under Office of Naval Research Contract N0001401MP20022.

References

Ebert, E. E., J. L. Schramm, and J. A. Curry, Disposition of solar radiation in sea ice and the upper ocean, *J. Geophys. Res.*, *100*, 15,965–15,975, 1995.
Maykut, G. A., and N. Untersteiner, Some results from a time dependent, thermodynamic model of sea ice, *J. Geophys. Res.*, *76*, 1550–1575, 1971.
Maykut, G. A., The surface heat and mass balance, *The Geophysics of Sea Ice*, edited by N. Untersteiner, 395–465, Plenum Press, 1986.
Maykut, G. A., and M. G. McPhee, Solar heating of the Arctic mixed layer, *J. Geophys. Res.*, *100*, 24,691–24,703, 1995.
McPhee, M. G., Turbulent heat flux in the upper ocean under sea ice, *J. Geophys. Res.*, *97*, 5365–5379, 1992.
McPhee, M. G., and N. Untersteiner, Using sea ice to measure vertical heat flux in the ocean, *J. Geophys. Res.*, *87*, 2071–2074, 1982.
Moritz, R. E., J. A. Curry, A. S. Thorndike, and N. Untersteiner, *SHEBA, A Research Program on the Surface Heat Budget of the Arctic Ocean*, Arctic System Science: Ocean-Atmosphere-Ice Interactions Report Number 3, 34 pp, 1993.
Perovich, D. K., W. B. Tucker III, and R. A. Kirshfield, Oceanic heat flux in Fram Strait measured by a drifting buoy, *Geophys. Res. Let.*, *16*, 995–998, 1989.
Perovich, D. K., B. C. Elder, and J. A. Richter-Menge, Observations of the annual cycle of sea ice temperature and mass balance, *Geophys. Res. Let.*, *5*, 555–558, 1997.
Perovich, D. K., et al., Year on ice gives climate insights, *EOS, Trans. Amer. Geophys. Union*, *80*(481), 485–486, 1999.
Perovich, D. K., W. B. Tucker III, and K. A. Ligett, Aerial observations of the evolution of ice surface conditions during summer, *J. Geophys. Res.*, in press.
Perovich, D. K., T. C. Grenfell, J. A. Richter-Menge, B. Light, W. B. Tucker III, and H. Eicken, Thin and thinner: Ice mass balance measurements during SHEBA, *J. Geophys. Res.*, in press.
Richter-Menge, J., D. Perovich, and S. Pegau, The impact of summer ice dynamics on the surface heat budget of the Arctic Ocean, *Ann. Glaciol.*, *33*, 201–206, 2001.
Schwerdtfeger, P., The thermal properties of sea ice, *J. Glaciol.*, *4*, 789–807, 1963.
Untersteiner, N., On the mass and heat budget of Arctic sea ice, *Arch. Meteorol. Geophys. Bioklim., Ser. A*, *12*, 151–182, 1961.
Uttal, T., et al., Surface Heat Budget of the Arctic Ocean, *Bull. Amer. Meteor. Soc.*, *83*, 255–275, 2002.
Wettlaufer, J. S. , Heat flux at the ice-ocean interface, *J. Geophys. Res.*, *96*, 7215–7236, 1991.

D. K. Perovich and B. Elder, ERDC-CRREL, 72 Lyme Road, Hanover, NH 03755, USA.